

Original Article

# Comparative Analysis on Reinforced Concrete Beam-Column Joint with Sisal Fiber Under Cyclic Loading

R. Abirami<sup>1</sup>, S. P. Sangeetha<sup>2</sup>, R. Divahar<sup>3</sup>

<sup>1,2,3</sup>Department of Civil Engineering, Aarupadai Veedu Institute of Technology, Vinayaka Mission's Research Foundation, (Deemed to be University), Tamil Nadu, India.

<sup>1</sup>Corresponding Author : abirajan26@gmail.com

Received: 26 March 2023

Revised: 21 May 2023

Accepted: 09 June 2023

Published: 30 June 2023

**Abstract** - The most critical failure regions are the joints between beams and columns. Under dynamic loads, the bonding of the rebars in the concrete will be severely stressed and fail. In addition to damaging the column loading paths, the collapse of the joint point may also affect the structure's overall ductility and capacity to dissipate energy. This study examined the relationship between natural fiber in beam-column joints by adding 0.5% to 1.5% with an increment of 0.25% of sisal fiber to reinforced concrete. Ductile detailing was done as per the IS 13920-2016. The analysis is carried out using the finite element software ANSYS workbench, and it is developed considering the effects of cyclic loading. The structural behaviour under cyclic loading was analyzed using Finite Element Method (FEM) analysis, including maximum load and displacement values compared with experimental values. A Comparison of FEM analysis and experimental values showed that the 1.25 % addition of Sisal fiber in reinforced concrete performs better in the joint between a beam and a column to withstand lateral and seismic loads on the structures.

**Keywords** - Beam column joint, Sisal fiber, Cyclic loading, FEM analysis, Displacement, ANSYS.

## 1. Introduction

In reinforced concrete structures in earthquake-prone areas, the beam-column joints are frequently regarded as a crucial component [1, 2]. Using closely spaced hoops as transverse reinforcement was suggested to provide the beam-column junction appropriate ductility [3]. Numerous researchers have tried to ease the technical challenges by reducing the joint reinforcement layout [4]. Fiber-reinforced concrete is favoured since this results in congestion and makes it harder to consolidate concrete in the joints [5]. The use of NaturalFiberReinforcedConcrete (NFRC) as extra reinforcement rather than compressing stirrups in the beam-column joints was suggested in various experimental tests.

Existing beam-column assemblages of framed buildings were typically built to act in a weak column-strong beam way [6]. This can lead to local hinges in the column when the building is subjected to seismic pressures. Adapting existing beam-column assemblages to operate in a weak column-strong beam fashion makes it possible to circumvent this issue and save time and money [7]. The structural integrity of the building may be jeopardised as a result of this pattern of behaviour. The associated failure mode, which a brittle structural failure can identify, thus reflects the lower bound of the hierarchy of strength and is the mode of failure connected to it [8, 9]. It is further distinguished because it is

the only failure mode with a brittle structural collapse. The fact that this failure mode is the mode of failure that is linked with it is one way to recognise it [10, 11].

Epoxy repair, elimination and replacement of weakened concrete strengthened or Prestressed Concrete (PC) jacketing, construction unit wrapping or partial masonry infill, steel jacketing and addition to external steel elements, along with applications using Fiber-Reinforced Polymer (FRP) materials are some of the fixes and enhancing techniques that have been studied in the literature [12, 13]. Other techniques include applications using steel jacketing and adding external steel elements. The installation of outside steel elements, masonry unit jacketing, partial masonry infill, steel jacketing, and masonry unit jacketing combined with steel jacketing are some other techniques [14, 15]. Each strategy necessitates a particular level of creative sophistication, in addition to the labour expense, range of applicability, and disturbance of building occupancy that must be meticulously considered [16].

Based on a thorough review of the literature, it is known that only a tiny amount of research has been published on the small-scale behaviour of experiments, square RC columns wrapped in Glass Fiber Reinforced Polymer(GFRP) that have different corner angles. The control specimens were



three columns that had been unwrapped. Three columns were covered with one and two layers of GFRP, with each column's angle corners corresponding to a 25 mm cover. The GFRP-wrapped columns endured more significant axial displacement than the control column to increase their compressive strength [17, 18].

## 2. Analytical Investigation

### 2.1. Modeling

An ANSYS programme was applied to conduct FiniteElementAnalysis (FEA) of the joint between the beam and the column while it had been exposed to cyclic loading. This was done to determine how the joint would react to the loading conditions. During the nonlinear static analysis carried out on the specimens of the connection joint using the FEA, the samples' materials and geometric nonlinearities are considered. This ensures that the analysis is accurate. The total specified loads applied to a body of finite components will be divided into a number that are distinct load increments in a nonlinear analysis. This will ensure that the body can withstand the stipulated loads. After each increment, the structure is very close to being in equilibrium, and the structure's stiffness matrix will be adjusted to reflect any nonlinear changes that may have occurred in the structure's total stiffness [19].

#### 2.1.1. Element

For the concrete elements throughout the whole geometry in the external connection specimens depicted in Figure 1, a uniform mesh size of 10 mm was selected. Steel bars are used with reinforcement mesh of the same size. The connection has 15246 elements and 32461 nodes with this design.

#### 2.1.2. Loading and Boundary Condition

Figure 2 details the shape and boundary circumstances of the RC beam-column connections used with FEM analysis. In the first step, the column top surface is subjected to a compressive axial load constant throughout the analysis. In the second step, the specimen receives monotonic lateral loading from the beam's end surface.

#### 2.1.3. Material Specification

Concrete compressive and tensile strengths, Poisson's ratio, and Young's modulus of elasticity ( $E_c$ ) are the concrete material parameters used in the analysis provided in Table 1. Experimental measurements of the poisson's ratio value for concrete material are made and used. With Young's modulus of  $2 \times 10^5$  MPa and a Poisson's ratio of 0.28, steel reinforcement exhibited elastic uniaxial tensile stress-strain behaviour.

#### 2.1.4. Reinforcement Details

Twelve specimens of cross sections of the external beam-column joints with a beam span of 1.5 metres and a

column height of 1 metre were cast. The beams had dimensions of 200 mm by 150 mm, and the columns had dimensions of 150 mm by 150 mm. Each specimen has reinforcement detailing that adheres to the standards established by IS456-2000, as well as detailing that adheres to the standards established by IS13920-1993. Reinforcement can be provided in bars ranging from 4 to 12 mm in diameter and stirrups of 8 mm in diameter uniformly spaced 120 mm from centre to centre. The anchorage zones of the beam and the column each have tensile reinforcement at the connection for 8 mm stirrups, and the spacing between them ranges from 75 mm to 300 mm. The strengthening features of the beam-column junction are illustrated in Figure 3.

The experiment setup consists of a response frame, a hydraulic actuator with a power of 400kN and 100 mm stroke length, with a frame load capacity of 50 KN, applying loads to the test specimens using a hydraulic jack shown in Figure 4. In the column's uppermost part, Linear Variable Differential Transducers (LVDT) were employed to monitor lateral displacement, and one load cell linked to the actuator was utilised to record cyclic lateral loads.

## 3. FEM Analysis Results

Figure 5 depicts the connections vulnerable to lateral loading between RC beams and columns. These connections are indicated in Figure 5. The load-displacement curves that are monitored at the specimen joint serve the purpose of providing a representation of the FEA results for these connections. This is done in order to provide an accurate depiction of the results [20-23].

## 4. Results and Discussion

Table 2 displays the maximum lateral loads and displacements determined by experimental test results and shown by numerical modelling.

Figure 6 compares the simulation-predicted load-displacement curves with the experimental results of beam-column joint specimens. In comparison to the control specimens, the ultimate strength of CCBCJ 01, SFBCJ 0.5, SFBCJ 0.75, SFBCJ 1, SFBCJ 1.25 and SFBCJ 1.5 increased by 6%, 23%, 28%, 34%, and 17%, respectively, after the FEA method. For all specimens, a comparable rise in deflections was observed.

According to the finite element analysis's observations, the post-yield behaviour somewhat deviates from the initial reaction, like the test results [24]. This may be caused by the impacts of a few a priori assumptions, like the choice of concrete's compressive and tensile properties, the inherent differences between the presence and orientation of fibers, and the uncertainties frequently associated with experimental efforts [25, 26].

**4.1. Comparison of Damage Index Vs Number of Cycles**

Figure 7 depicts all test specimens' cumulative damage index values from FEM analysis. A widely used damage index for aspects of reinforced concrete was proposed [27], defined as a linear equation of the standardized maximum deflection and the normalization hysteretic energy, as shown below.

$$D = \frac{\delta_m}{\delta_u} + \frac{\beta}{F_y \delta_u} \int dE \tag{1}$$

$\delta_m$  denotes the optimum deformation caused by seismic forces and is the optimum deformation under cyclic loads,  $F_y$  is the yield strength,  $dE$  is hysteretic energy absorbed incrementally, and  $\beta$  is the effect of cyclic loading on structural damage. The damage index is such a normalized quantity with a value that must be between zero to one. D.I = 0 indicates an undamaged, i.e. earthquake-induced elastic limit behaviour of the structure, whereas the index of damage value one denotes structural failure, i.e. general failure of the structure.

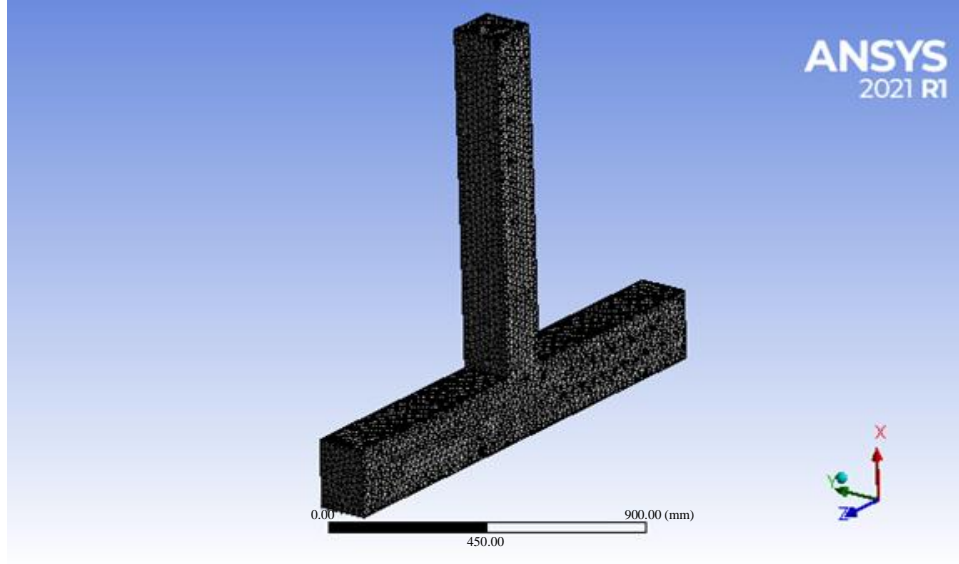


**Fig. 1 Concrete element mesh of exterior connection**

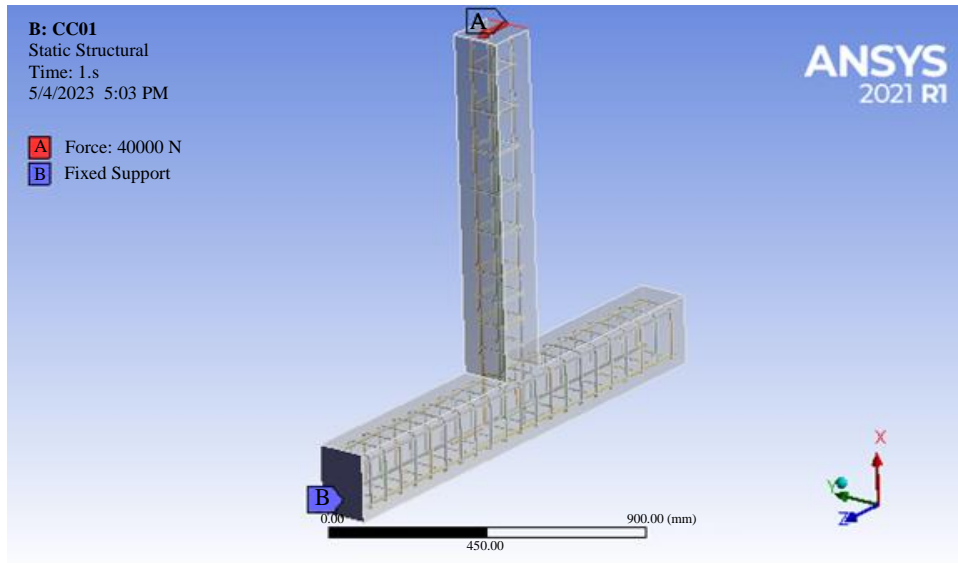


**Fig. 2 Reinforcement details of the exterior connection**

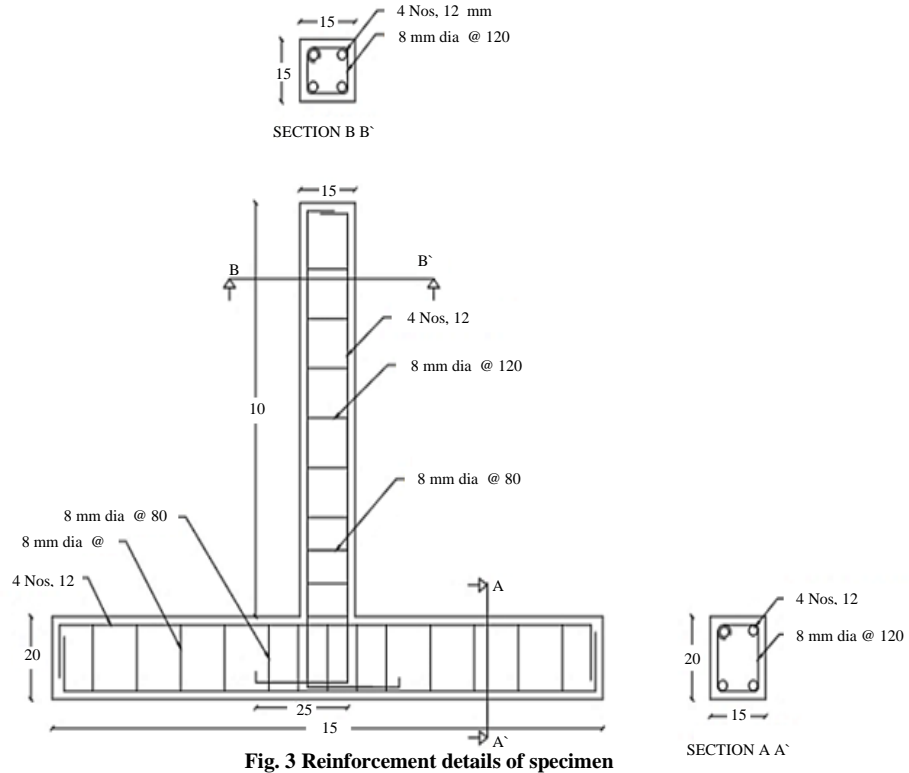
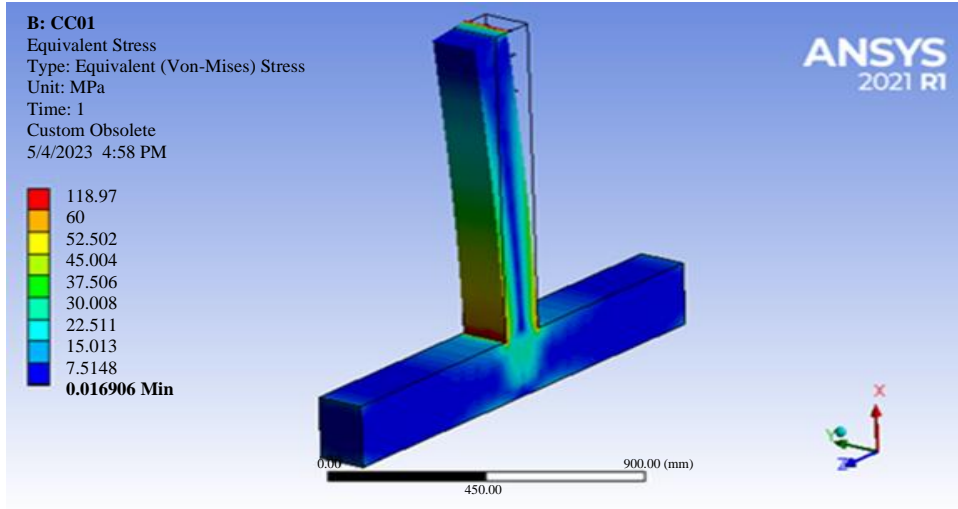


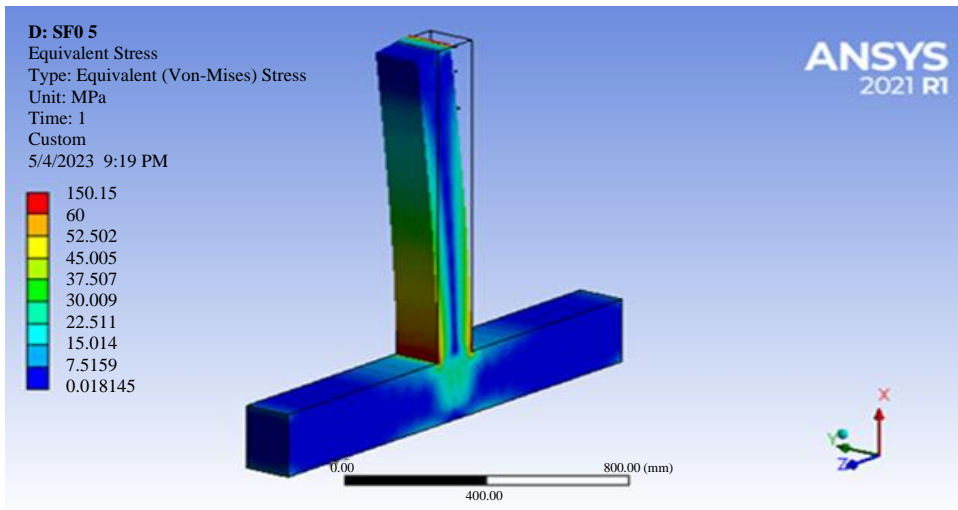
Fig. 3 Reinforcement details of specimen



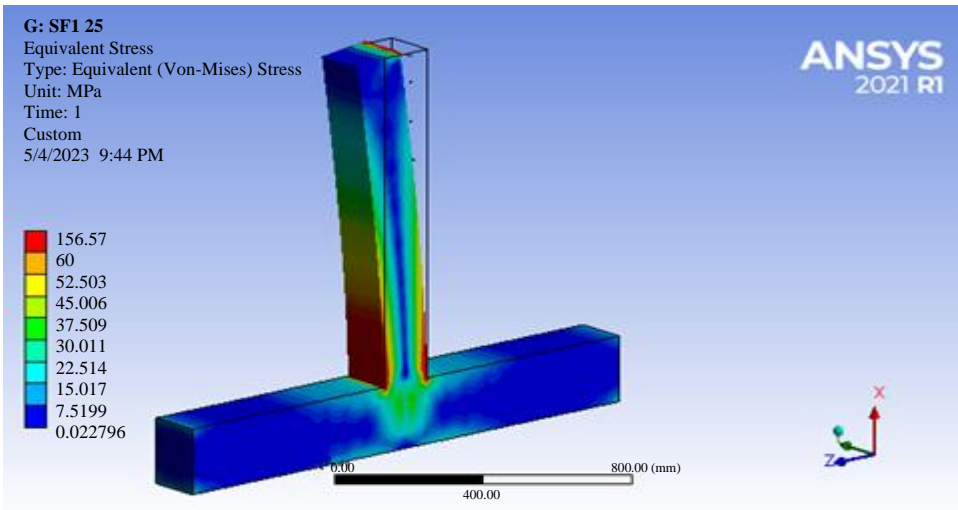
Fig. 4 Experimental setup for the beam-column joint



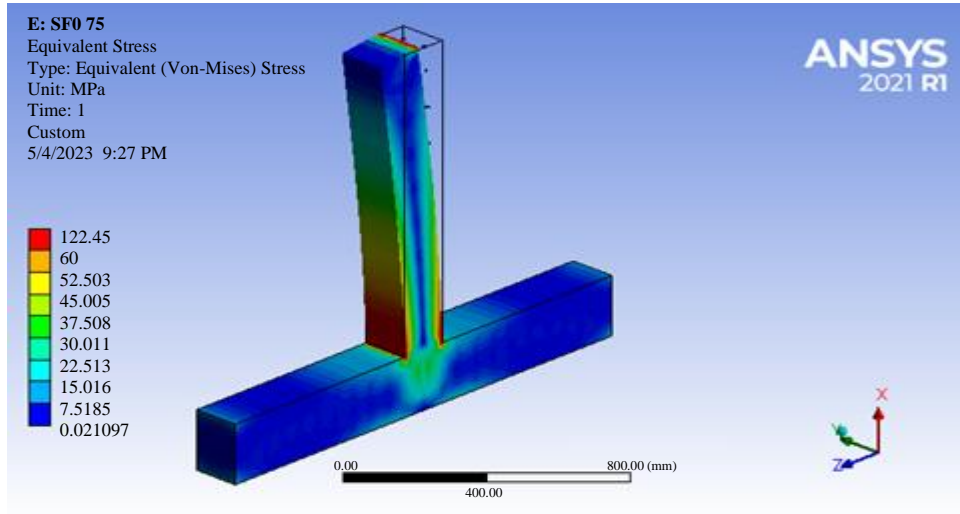
(a)



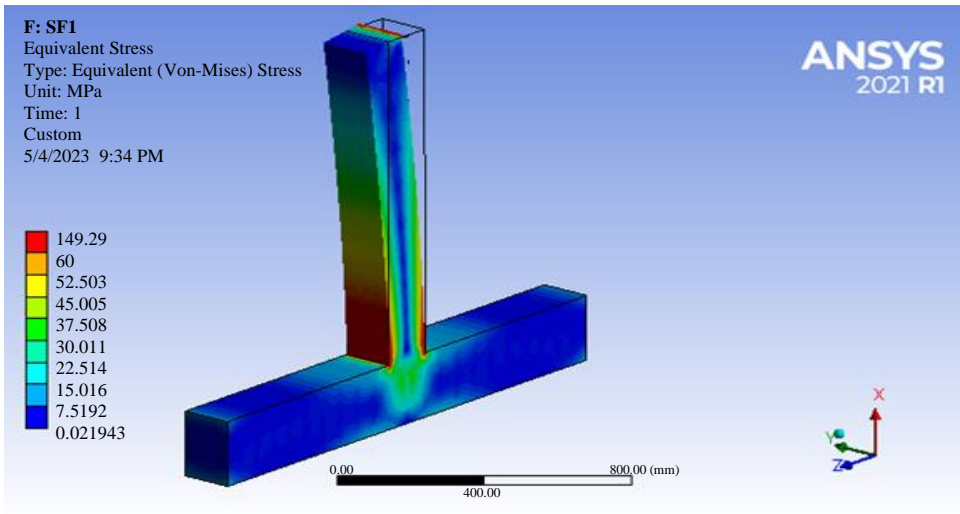
(b)



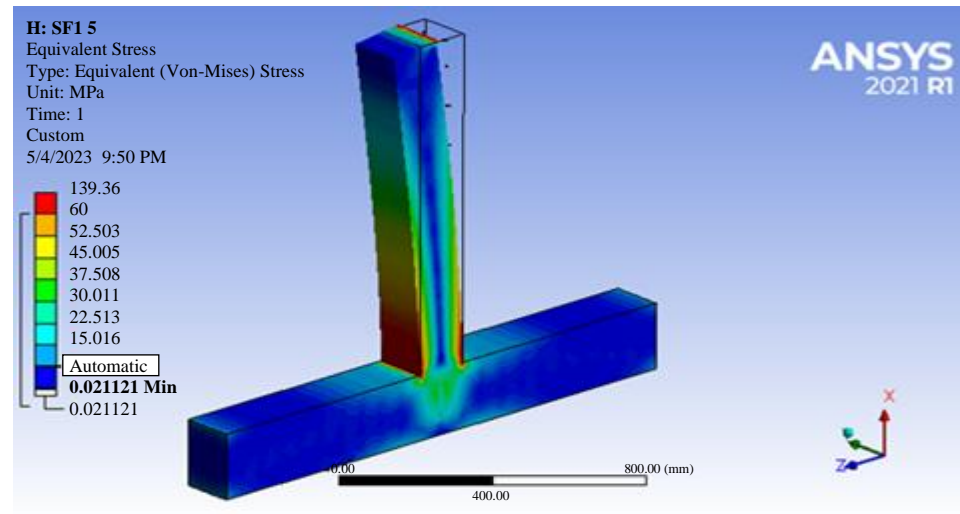
(c)



(d)



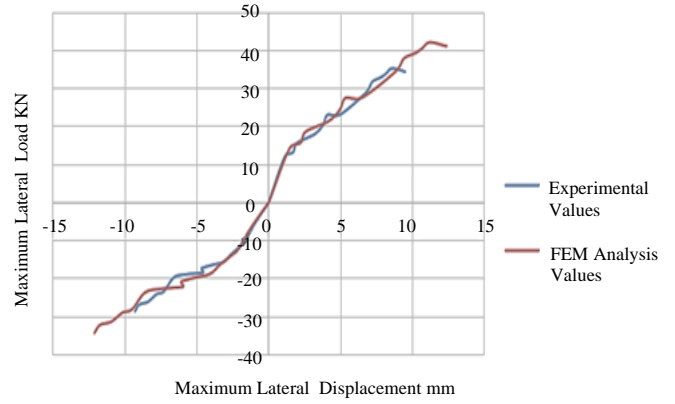
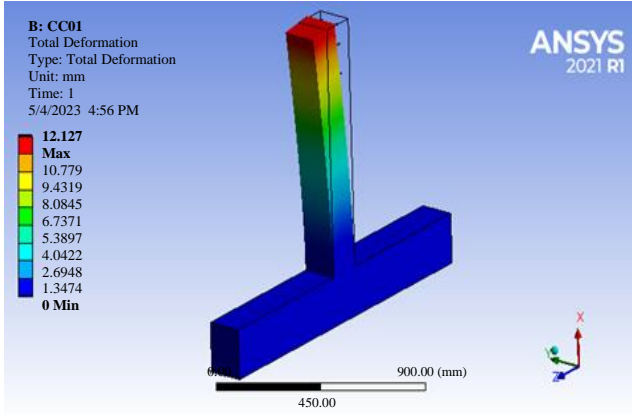
(e)



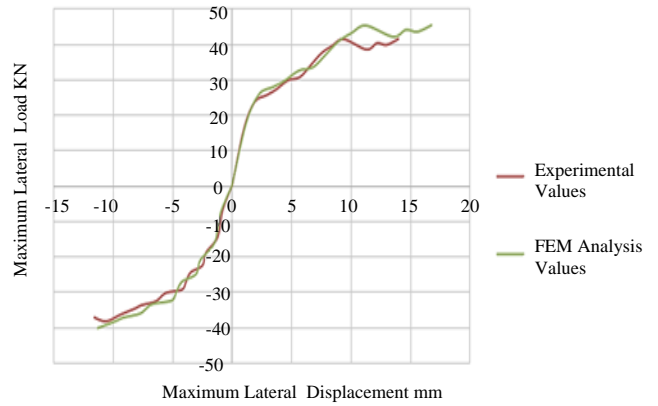
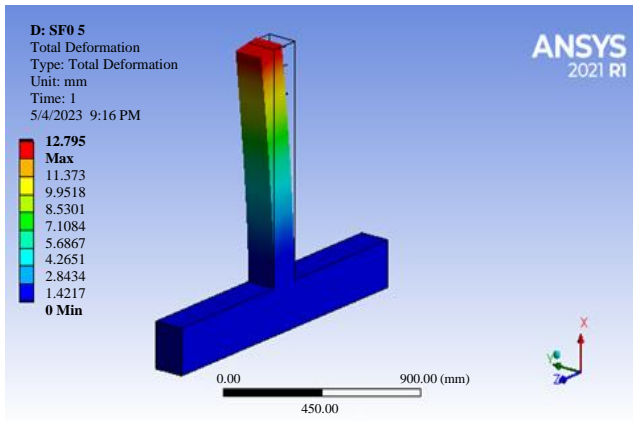
(f)

Fig. 5 (a) CCBCJ 01, (b) SFBCJ 0.5, (c) SFBCJ 0.75, (d) SFBCJ 1, (e) SFBCJ 1.25, (f) SFBCJ 1.5 Lateral load and displacement obtained from FEM

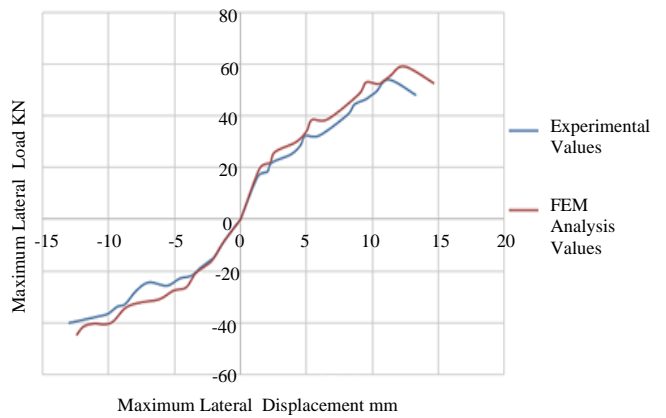
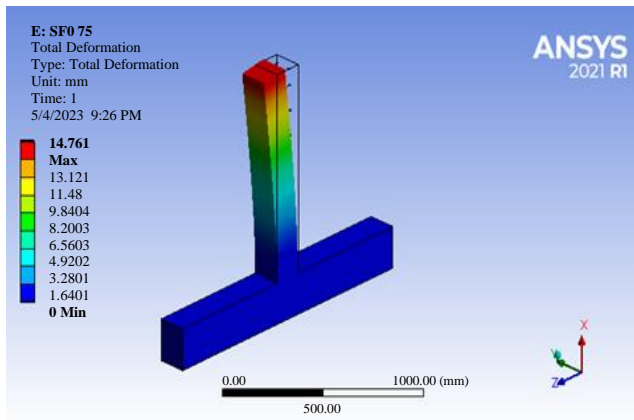




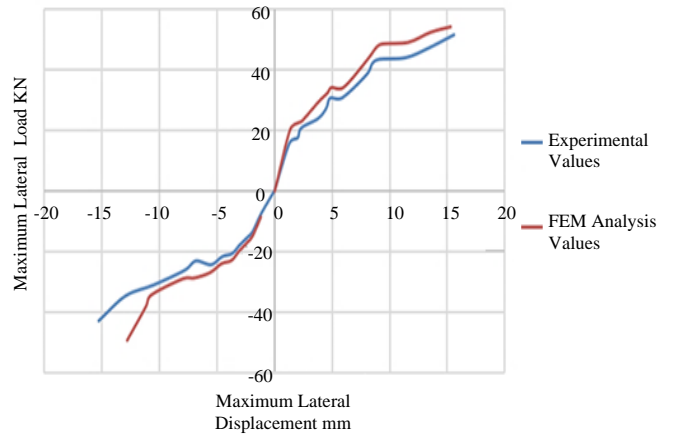
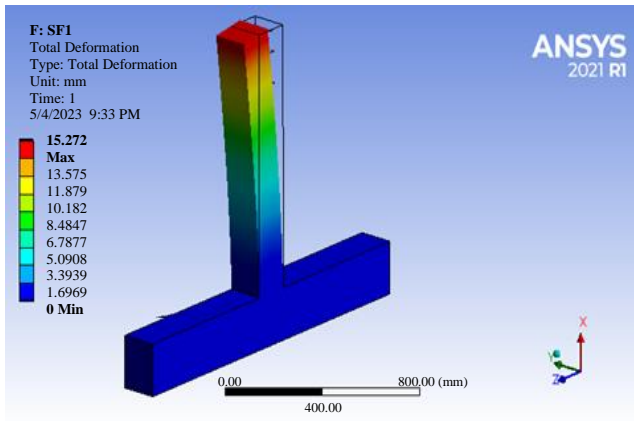
(a) Maximum displacement - CCBCJ 01



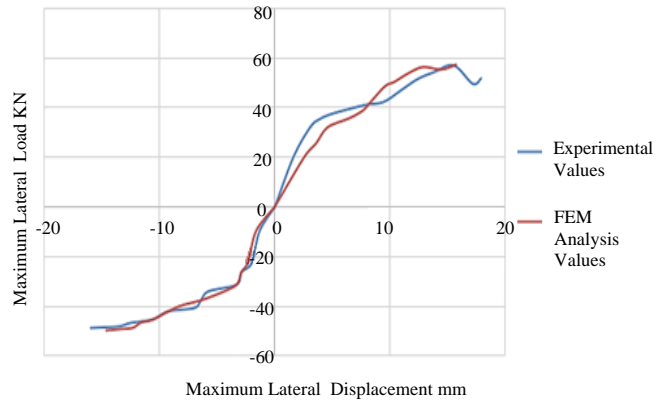
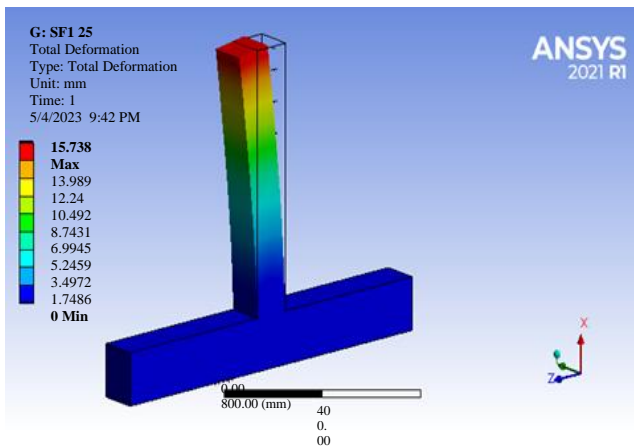
(b) Maximum displacement - SFBCJ 0.5



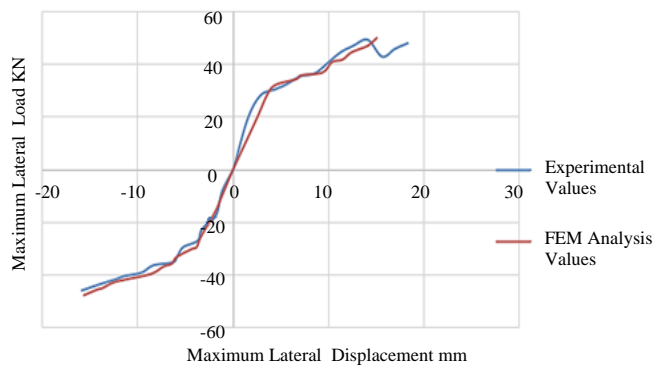
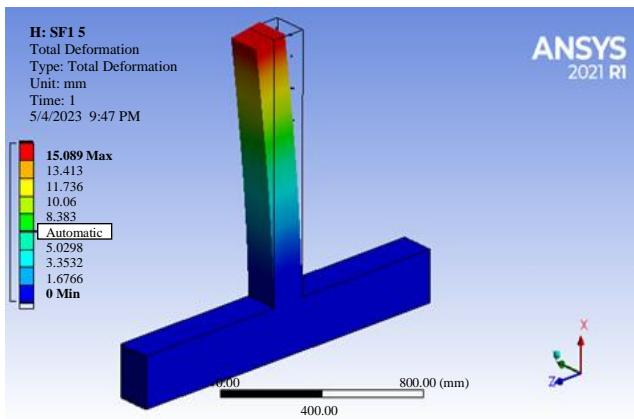
(c) Maximum displacement - SFBCJ 0.75



(d) Maximum displacement - SFBCJ 1



(e) Maximum displacement - SFBCJ 1.25



(f) Maximum displacement - SFBCJ 1.5

Fig. 6 (a), (b), (c), (d), (e), (f) Comparison of experimental values vs FEM analysis values



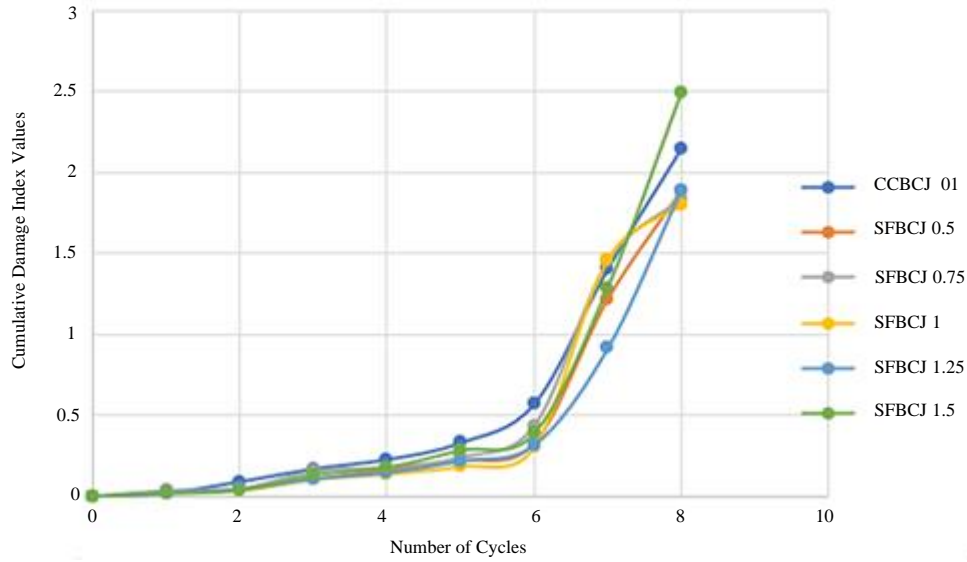


Fig. 7 Cumulative damage index vs number of cycles

Table 1. Input concrete properties

Sl. No	Specimen ID	Compressive Strength at 28days N/mm <sup>2</sup>	Young's Modulus Ec GPa	Poisson Ratio of concrete( $\nu$ )
1	CCBCJ	32.75	28.613	0.189
2	SFBCJ 0.5	34.15	29.219	0.190
3	SFBCJ 0.75	34.78	29.48	0.191
4	SFBCJ 1	35.17	29.65	0.191
5	SFBCJ 1.25	35.78	29.908	0.192
6	SFBCJ 1.5	33.10	28.76	0.192

Table 2. Comparison of experimental vs finite element analysis values at peak loads (PL)

S. No	Specimens	Experimental Value				Finite Element Analysis Value			
		Lateral PL in KN	Displacement at PL in mm	Lateral PL in KN	Displacement at PL in mm	Lateral PL in KN	Displacement at PL in mm	Lateral PL in KN	Displacement at PL in mm
		+ Ve	+Ve	-Ve	-Ve	+ Ve	+Ve	-Ve	-Ve
1	CCBCJ 01	38.6	9.5	28.6	7.91	42.6	12.12	34.32	11.10
2	SFBCJ 0.5	41.4	11.2	37.2	10.1	45.4	12.75	41.49	11.21
3	SFBCJ 0.75	48.02	13.3	40.04	11.07	52.6	14.76	44.4	12.4
4	SFBCJ 1	50.74	15.88	48.62	13.56	54.12	15.27	49.18	12.8
5	SFBCJ 1.25	51.85	17.58	49.09	12.96	57.4	15.78	52.6	13.8
6	SFBCJ 1.5	48.25	18.3	47.47	14.45	50.26	15.08	49.7	14.12

## 5. Conclusion

In the present study, experimental and numerical analyses were utilised to assess the performance of exterior beam-column joints reinforced with sisal fiber.

- All specimens with fibers had higher ultimate loads than the control specimen. The specimen with 1.25% sisal fiber had the highest forward cycle peak load of 57.2 KN. The specimen with 1.25% sisal fiber had the highest reverse cycle peak load, 52.6 KN. It had the highest peak load overall. The specimen with sisal fiber had a higher peak load due to good fiber distribution and crack bridging, which inhibited crack development.
- The study and experiment showed that adding 1.25% sisal fiber to reinforced concrete at the junction increases the ductility of RCC external beam-column joints.

- According to the analytical investigation, adding sisal fiber reinforcement boosted joints' ultimate load-carrying capability and ductility under both upward and downward loading circumstances.

## Future Research

Future studies must consider the torsional effects of slab inclusion or beam eccentricities on joint resistance. Investigations of the behaviour BCJs are also necessary to draw attention to the likelihood of untypical failures.

## Acknowledgements

The authors are obliged to Aarupadai Veedu Institute of Technology, Vinayaka Mission's Research Foundation, for providing laboratory facilities.

## References

- [1] Mohamed Hasaballa, and Ehab El-Salakawy, "Shear Capacity of Exterior Beam-Column Joints Reinforced with GFRP Bars and Stirrups," *Journal of Composites for Construction*, vol. 20, no. 2, 2016. [[CrossRef](#)] [[Google Scholar](#)] [[Publisher Link](#)]
- [2] N. Dharmesh, and L. Govindaraju, "A Study on Shear Frame Structure by Modal Superposition Method," *International Journal of Engineering Trends and Technology*, vol. 71, no. 2, pp. 457-465, 2023. [[CrossRef](#)] [[Publisher Link](#)]
- [3] S. Y. Laseima et al., "Seismic Behavior of Exterior RC Beam-Column Joints Retrofitted using CFRP Sheets," *Latin American Journal of Solids and Structures*, vol.17, pp. 124-129, 2020. [[CrossRef](#)] [[Google Scholar](#)] [[Publisher Link](#)]
- [4] Kien Le-Trung et al., "Experimental Study of RC Beam-Column Joints Strengthened using CFRP Composites," *Composites Part B: Engineering*, vol. 41, no. 1, pp. 76-85, 2010. [[CrossRef](#)] [[Google Scholar](#)] [[Publisher Link](#)]
- [5] Abhijit Mukherjee, and Mangesh Joshi, "FRPC Reinforced Concrete Beam-Column Joints under Cyclic Excitation," *Composite Structures*, vol. 70, no. 2, pp. 185-199, 2005. [[CrossRef](#)] [[Google Scholar](#)] [[Publisher Link](#)]
- [6] R. Siva Chidambaram, and Pankaj Agarwal, "Seismic Behavior of Hybrid Fiber Reinforced Cementitious Composite Beam-Column Joints," *Materials & Design*, vol. 86, pp. 771-781, 2015. [[CrossRef](#)] [[Google Scholar](#)] [[Publisher Link](#)]
- [7] Abass Abayomi Okeola, John Mwero, and Abdulhafeez Bello, "Behavior of Sisal Fiber-Reinforced Concrete in Exterior Beam-Column Joint under Monotonic Loading," *Asian Journal of Civil Engineering*, vol. 22, pp. 627-636, 2021. [[CrossRef](#)] [[Google Scholar](#)] [[Publisher Link](#)]
- [8] Roberto Realfonzo, Annalisa Napoli, and Joaquín Guillermo Ruiz Pinilla, "Cyclic Behavior of RC Beam-Column Joints Strengthened with FRP Systems," *Construction and Building Materials*, vol. 54, pp. 282-297, 2014. [[CrossRef](#)] [[Google Scholar](#)] [[Publisher Link](#)]
- [9] Samala Haricharan, and R. Swami Ranga Reddy, "Modeling and Analysis of Reinforced Concrete Beam Without Transverse Reinforcement and Strengthened with CFRP Lamellas: A Parametric Study," *SSRG International Journal of Civil Engineering*, vol. 7, no. 7, pp. 123-127, 2020. [[CrossRef](#)] [[Publisher Link](#)]
- [10] B. Venkatesan et al., "Finite Element Analysis (FEA) for the Beam-Column Joint Subjected to Cyclic Loading was Performed using ANSYS," *Circuits and Systems*, vol. 7, no. 8, 2016. [[CrossRef](#)] [[Google Scholar](#)] [[Publisher Link](#)]
- [11] Ammar Yaser Ali, and Ali Abdulameer Al-Rammahi, "Flexural Behavior of Hybrid-Reinforced Concrete Exterior Beam-Column Joints under Static and Cyclic Loads," *Fibers*, vol. 7, no.10, 2019. [[CrossRef](#)] [[Google Scholar](#)] [[Publisher Link](#)]
- [12] K. Padmanabham, and L. Jaygadeep Sai, "Experimental Study on RC Exterior Beam-Column Joint Retrofitted by Post Installation Technique," *SSRG International Journal of Civil Engineering*, vol. 9, no.12, pp. 7-20, 2022. [[CrossRef](#)] [[Google Scholar](#)] [[Publisher Link](#)]
- [13] W. T. Lee, Y. J. Chiou, and M. H. Shih, "Reinforced Concrete Beam-Column Joint Strengthened with Carbon Fiber Reinforced Polymer," *Composite Structures*, vol. 92, no.1, pp. 48-60, 2010. [[CrossRef](#)] [[Google Scholar](#)] [[Publisher Link](#)]
- [14] Gia Toai Truong et al., "Seismic Performance of Exterior RC Beam-Column Joints Retrofitted using Various Retrofit Solutions," *International Journal of Concrete Structures and Materials*, vol. 11, pp. 415-433, 2017. [[CrossRef](#)] [[Google Scholar](#)] [[Publisher Link](#)]
- [15] N. Dharmesh, and L. Govindaraju, "Sensitivity Analysis of RC Beam under Flexure and Shear by FOSM Method," *International Journal of Engineering Trends and Technology*, vol. 71, no. 1, pp. 141-151, 2023. [[CrossRef](#)] [[Publisher Link](#)]
- [16] M. J. Shannag, S. Barakat, and M. Abdul-Kareem, "Cyclic Behavior of HPFRC-Repaired Reinforced Concrete Interior Beam-Column Joints," *Materials and Structures*, vol. 35, pp. 348-356, 2002. [[CrossRef](#)] [[Google Scholar](#)] [[Publisher Link](#)]

- [17] S. M. Leela Bharathi, and M. Kumar, “An Experimental Study on the Flexural Behaviour of Natural Fibre Reinforced Concrete with Partial Replacement of Flyash and GGBS,” *SSRG International Journal of Civil Engineering*, vol. 6, no. 4, pp. 46-49, 2019. [[CrossRef](#)] [[Google Scholar](#)] [[Publisher Link](#)]
- [18] S. Nallusamy, and A. Karthikeyan, “Synthesis and Wear Characterization of Reinforced Glass Fiber Polymer Composites with Epoxy Resin using Granite Powder,” *Journal of Nano Research*, vol. 49, no. 1, pp. 1-9, 2017. [[CrossRef](#)] [[Google Scholar](#)] [[Publisher Link](#)]
- [19] N. Ganesan, P. V. Indira, and M.V. Sabeena, “Behaviour of Hybrid Fibre Reinforced Concrete Beam–Column Joints under Reverse Cyclic Loads,” *Materials & Design (1980-2015)*, vol. 54, pp. 686-693, 2014. [[CrossRef](#)] [[Google Scholar](#)] [[Publisher Link](#)]
- [20] Flora Faleschini et al., “Experimental Behavior of Beam-Column Joints Made with EAF Concrete Under Cyclic Loading,” *Engineering Structures*, vol. 139, pp. 81-95, 2017. [[CrossRef](#)] [[Google Scholar](#)] [[Publisher Link](#)]
- [21] R. Tuğrul ERDEM et al., “Impact Analysis of a Concrete Beam via Generative Adversarial Networks,” *International Journal of Recent Engineering Science*, vol. 9, no. 1, pp. 16-21, 2022. [[CrossRef](#)] [[Publisher Link](#)]
- [22] Hassan Bagheri, and Kouros Mirzaie, “Predicting the Response of Concrete Columns to Eccentric Loading using Finite Element Analysis,” *SSRG International Journal of Civil Engineering*, vol. 10, no. 4, pp. 1-7, 2023. [[CrossRef](#)] [[Google Scholar](#)] [[Publisher Link](#)]
- [23] Norashidah Abd Rahman et al., “Performance of Modified Foam Concrete-Filled Column Hollow Sections,” *International Journal of Engineering Trends and Technology*, vol. 70, no. 7, pp. 399-404, 2022. [[CrossRef](#)] [[Google Scholar](#)] [[Publisher Link](#)]
- [24] Prasad Bishetti et al., “Glass Fiber Reinforced Concrete,” *SSRG International Journal of Civil Engineering*, vol. 6, no. 6, pp. 23-26, 2019. [[CrossRef](#)] [[Publisher Link](#)]
- [25] Usha Sivasankaran, Seetha Raman, and S. Nallusamy, “Experimental Analysis of Mechanical Properties on Concrete with Nano Silica Additive,” *Journal of Nano Research*, vol. 57, pp. 93-104, 2019. [[CrossRef](#)] [[Google Scholar](#)] [[Publisher Link](#)]
- [26] Mohamed Saad Abbadi, and Nouzha Lamdouar, “Seismic Performance Limit States Assessment of Bridge Piers by Numerical Analysis and Experimental Damage Observations,” *International Journal of Engineering Trends and Technology*, vol. 69, no. 10, pp. 168-177, 2021. [[CrossRef](#)] [[Publisher Link](#)]
- [27] Young-Ji Park et al., “Seismic Damage Analysis of Reinforced Concrete Buildings,” *Journal of Structural Engineering*, vol. 111, no.4, pp. 740-757, 1985. [[CrossRef](#)] [[Publisher Link](#)]